Inorganic Chemistry

Article

Spontaneous Self-Assembly of an Unsymmetric Trinuclear Triangular Copper(II) Pyrazolate Complex, [Cu₃(μ₃-OH)(μ-pz)₃(MeCOO)₂(Hpz)] (Hpz = Pyrazole). Synthesis, Experimental and Theoretical Characterization, Reactivity, and Catalytic Activity

Maurizio Casarin,[†] Carlo Corvaja,[†] Corrado di Nicola,[‡] Daniele Falcomer,[†] Lorenzo Franco,[†] Magda Monari,[§] Luciano Pandolfo,*,[†] Claudio Pettinari,*,[‡] Fabio Piccinelli,[§] and Pietro Tagliatesta[∥]

Department of Chemical Sciences, University of Padova, Via Marzolo 1, I-35131 Padova, Department of Chemical Sciences, University of Camerino, Via S. Agostino 1, I-62032 Camerino (MC), Department of Chemistry "G. Ciamician", University of Bologna, Via Selmi 2, I-40126 Bologna, and Department of Chemical Sciences and Technologies, University of Roma Tor-Vergata, Via della Ricerca Scientifica, I-00133 Roma, Italy

The almost quantitative formation of the triangular trinuclear copper derivative [Cu₃(μ₃-OH)(μ-pz)₃(MeCOO)₂(Hpz)] (**1**) (Hpz = pyrazole), has been simply achieved by adding Hpz to an ethanol solution of Cu(MeCOO)₂·H₂O. An X-ray molecular structure determination shows that **1** is completely unsymmetric and that trinuclear units result assembled in an extended bidimensional network formed through acetate bridges and hydrogen bonds. EPR and magnetic measurements are consistent with the presence of a single unpaired electron. Theoretical density functional calculations carried out for $S = 1/2$ provide a thorough description of the electronic structure of **1**, allowing a detailed assignment of its UV–vis absorption spectrum. Compound **1** reacts with MeONa, yielding [Cu₃(μ₃-OH)-(μ-pz)₃(MeCOO)(MeO)(Hpz)] (**2**) and [Cu₃(μ₃-OH)(μ-pz)₃(MeO)₂(Hpz)] (**3**) through the substitution of one and two acetate ions, respectively, with MeO⁻ ion(s). The spontaneous self-assembly of the triangular trinuclear Cu₃ moiety seems to occur only with pyrazole as can be inferred by the results obtained in the reactions of copper(II) acetate with some substituted pyrazoles leading to the formation of mononuclear [Cu(MeCOO)₂(L)₂] (**4**–**8**) and dinuclear [Cu(MeCOO)₂(L)]₂ (**9**–**11**) (L = substituted pyrazole) compounds. Also the presence of acetate ions seems to play a leading role in determining the formation of the trinuclear triangular arrangement, as indicated by the formation of a mononuclear derivative, [Cu(CF₃COO)₂(Hpz)]₂ (compound **12**), in the reaction of copper(II) trifluoroacetate with pyrazole. Compounds **1**–**3**, as well as some other mono- and dinuclear copper(II)-substituted pyrazole complexes, have been tested as catalyst precursors in cyclopropanation reaction, observing the formation of products in a *syn:anti* ratio opposite that normally reported.

Introduction

In recent years, investigations of trinuclear transition-metal complexes have had a great development due to the discovery of the fundamental role played by these metal systems in several catalytic biological processes.[1] Moreover, this kind of compound often provides the possibility to study magnetostructural correlations in mixed bridged systems as well as the opportunity of testing magnetic exchange models.[2] A trinuclear array of copper(II) may be essential functional units in a number of multicopper blue oxidases,[3] such as laccase and ascorbate oxidases, which catalyze the four-electron reduction of dioxygen to water with concomitant one-electron

* Authors to whom correspondence should be addressed. Phone: +39 049 8275157 (L.P.); +39 0737 402234 (C.P.). Fax: +39 049 8275161 (L.P.); +39 0737 637345 (C.P.). E-mail: luciano.pandolfo@unipd.it (L.P.); claudio.pettinari@unicam.it (C.P.).
† University of Padova.
‡ University of Camerino.
§ University of Bologna.
∥ University of Roma Tor-Vergata.

(1) For some reviews see: (a) Solomon, E. I.; Sundaram, U. M.; Machonkin, T. E. *Chem. Rev.* **1996**, *96*, 2563. (b) Kaim, W.; Rall, J. *Angew. Chem., Int. Ed. Engl.* **1996**, *35*, 43.

oxidation of a variety of substrates, such as ascorbate and polyphenols, and aromatic polyamines.[4] The fully oxidized active site of ascorbate oxidase has a triangular arrangement of copper(II) atoms with Cu–Cu separations ranging from 3.6 to 3.9 Å, with a hydroxide or an oxo group acting as a bridge between the two type-3 copper atoms. There are three histidine residues bonded to each copper, while the type-2 copper atom is bonded to three histidine molecules and one water molecule or hydroxide group.[5] The study of the reaction mechanisms involved in these and other biological metal arrays is complicated by the fact that metal centers are normally present in small amounts with respect to the "organic" environment. Moreover, problems of solubility and/or stability are often present. A possible strategy to gain information about such complicated systems could involve the synthesis and the study of low molecular weight model complexes having characteristics such as solubility and stability in most common solvents that make easier their study and electronic and structural features similar to those of more complex systems under examination.[6] Consequently, it is of importance to synthesize low molecular weight trinuclear copper(II) complexes having a triangular arrangement of metal atoms and to study the conditions leading these compounds to mimic the behavior of natural products. Trinuclear triangular and chains of trinuclear triangular copper complexes, with[2b,d,e,7] or without[8] a $Cu_3(\mu_3\text{-OH})$, core have been reported, and Cole et al. synthesized and characterized a trinuclear triangular mixed-valence copper complex which exhibits "O_2 bond scission and intriguing structural, spectroscopic, and redox properties".[9]

Pyrazole and its derivatives are interesting ligands able to provide a 1,2-bridging form, often utilized to prevent

accumulation of positive charges in metal ion assembled compounds. Among the copper(II) systems, the linear trinuclear[10] one-dimensional chains,[10] two-dimensional triangular trinuclear networks,[11] and hexanuclear complexes[12] with triple pyrazolate bridges or containing small anions (such as Cl^-, OH^-, and N_3^-) as bridging units have been structurally characterized. Moreover, the unusual trinuclear Cu(II) species $[Cu_3(\mu_3\text{-OH})(\mu\text{-pz})_3(NO_3)_2(Hpz)_2]$ has been prepared from air oxidation of $[Cu(NO_3)(Hpz)_2]$ in the presence of moisture.[7a] In addition to that, there is an increasing interest in cyclic trinuclear metal complexes because these systems can be regarded as geometrically frustrated and offer the opportunity to test magnetic exchange models.[13]

Until the present work, no investigation of the reaction of copper(II) carboxylates with pyrazole had been reported. In the course of a research project dealing with the study of the interaction of copper carboxylates with azoles, by reacting pyrazole (hereafter Hpz) and $Cu(MeCOO)_2 \cdot H_2O$, we observed the formation of a previously unreported trinuclear triangular copper complex, $[Cu_3(\mu_3\text{-OH})(\mu\text{-pz})_3(MeCOO)_2\text{-}(Hpz)]$ (**1**).[14] Here we report a thorough description of its molecular and electronic structure coupled with experimental results obtained from IR, UV–vis, and EPR measurements. Moreover, data on the reactivity of **1** and some preliminary results about its catalytic behavior are presented. The syntheses and the characterization of a series of adducts obtained from the reaction of differently substituted pyrazoles with $Cu(MeCOO)_2 \cdot H_2O$ and from the reaction of Hpz with $Cu(CF_3COO)_2 \cdot 2H_2O$ are also reported and results seem to indicate that both pyrazole and acetate ion are determining in the self-assembly process of the trinuclear triangular Cu_3 moiety.

Experimental Section

Material and Methods. All chemicals were purchased from Aldrich and used without further purification. Elemental analyses (C, H, N, O) were performed with a Fisons Instruments 1108 CHNS-O elemental analyzer. IR spectra were recorded from 4000 to 100 cm^{-1} with a Perkin-Elmer system 2000 FT-IR instrument.

(2) (a) Kahn, O. *Chem. Phys. Lett.* **1997**, *265*, 109. (b) Ferrer, S.; Haasnoot, J. G.; Reedijk, J.; Muller, E.; Biagini Cingi, M.; Lanfranchi, M.; Manotti Lanfredi, A. M.; Ribas, J. *Inorg. Chem.* **2000**, *39*, 1859. (c) Gutierrez, L.; Alzuet, G.; Real, J. A.; Cano, J.; Borrás, J.; Castiñeiras, A. *Inorg. Chem.* **2000**, *39*, 3608. (d) Angaridis, P. A.; Baran, P.; Boa, R.; Cervantes-Lee, F.; Haase, W.; Mezei, G.; Raptis, R. G.; Werner, R. *Inorg. Chem.* **2002**, *41*, 2219. (e) Ferrer, S.; Lloret, F.; Bertomeu, I.; Alzuet, G.; Borrás, J.; Garcia-Granda, S.; Liu-Gonzales, M.; Haasnoot, J. G. *Inorg. Chem.* **2002**, *41*, 5821.

(3) Huber, R. *Angew. Chem.* **1989**, *101*, 849.

(4) Messerschmidt, A.; Ressi, A.; Ladenstein, R.; Huber, R.; Bolognesi, M.; Gatti, G.; Marchesini, A.; Finazzi-Agro, A. *J. Mol. Biol.* **1989**, *206*, 513.

(5) Suzuki, S.; Kataoka, K.; Yamaguchi, K. *Acc. Chem. Res.* **2000**, *33*, 728.

(6) Österberg, R. *Coord. Chem. Rev.* **1974**, *12*, 309.

(7) (a) Hulsbergen, F. B.; ten Hoedt, R. W. M.; Verschoor, G. C.; Reedijk, J.; Spek, A. L. *J. Chem. Soc., Dalton Trans.* **1983**, 539. (b) Angaroni, M.; Ardizzoia, G. A.; Beringhelli, T.; La Monica, G.; Gatteschi, D.; Masciocchi, N.; Moret, M. *J. Chem. Soc., Dalton Trans.* **1990**, 3305. (c) Sakai, K.; Yamada, Y.; Tsubomura, T.; Yabuki, M.; Yamaguchi, M. *Inorg. Chem.* **1996**, *35*, 542.

(8) (a) Jones, P. L.; Jeffery, J. C.; Maher, J. P.; McCleverty, J. A.; Rieger, P. H.; Ward, M. D. *Inorg. Chem.* **1997**, *36*, 3088. (b) Root, D. E.; Henson, M. J.; Machonkin, T.; Mukherjee, P.; Stack, T. D. P.; Solomon, E. I. *J. Am. Chem. Soc.* **1998**, *120*, 4982. (c) Setsune, J.-i.; Yokoyama, T.; Muraoka, S.; Huang, H.-w.; Sakurai, T. *Angew. Chem., Int. Ed.* **2000**, *39*, 1115. (d) Sanmartìn, J.; Bermejo, M. R.; Garcìa-Deibe, A. M.; Nascimento, O. R.; Lezama, L.; Rojo, T. *J. Chem. Soc., Dalton Trans.* **2002**, 1030. (e) López-Sandoval, H.; Contreras, R.; Escuer, A.; Vicente, R.; Bernès, S.; Nöth, H.; Leigh, G. J.; Barba-Behrens, N. *J. Chem. Soc., Dalton Trans.* **2002**, 2648. (f) Dong, G.; Chun-qi, Q.; Chun-ying, D.; Ke-liang, P.; Qing-jin, M. *Inorg. Chem.* **2003**, *42*, 2024.

(9) Cole, A. P.; Root, D. E.; Mukherjee, P.; Solomon, E. I.; Stack, T. D. P. *Science* **1996**, *273*, 1848.

(10) (a) Vos, G.; Haasnoot, J. G.; Verschoor, G. C.; Reedijk, J.; Schaminee, P. E. L. *Inorg. Chim. Acta* **1985**, *105*, 31. (b) Thomann, M.; Kahn, O.; Guilhem, J. Varret, F. *Inorg. Chem.* **1994**, *33*, 2433. (c) van Koningbruggen, P. J.; Haasnoot, J. G.; Vreugdenhil, W.; Reedijk, J.; Kahn, O. *Inorg. Chim. Acta* **1995**, 239, 5. (d) Kolnaar, J. J. A.; van Dijk, G.; Kooijman, H.; Spek, A.; Ksenofontov, V. G.; Gütlich, P.; Haasnoot, J. G.; Reedijk, J. *Inorg. Chem.* **1997**, *36*, 2433.

(11) (a) Chandrasekhar, V.; Kingsley, S. *Angew. Chem., Int. Ed.* **2000**, *39*, 2320. (b) Ardizzoia, G. A.; La Monica, G.; Cariati, F.; Cenini, S.; Moret, M.; Masciocchi, N. *Inorg. Chem.* **1991**, *30*, 4347.

(12) Sakai, K.; Yamada, Y.; Tsubomura, T.; Yabuki, M.; Yamaguchi, M. *Inorg. Chem.* **1996**, *35*, 542.

(13) (a) *Magnetic Molecular Materials*; Gatteschi, D., Kahn, O., Miller, J. S., Palacio, F., Eds.; Kluwer Academic: Dordrecht, The Netherlands, 1991. (b) Kahn, O.; Pei, Y.; Yournaux, Y. In *Inorganic Materials*; Bruce, D. W., O'Hare, O., Eds.; John Wiley & Sons: Chichester, U.K., 1992. (c) Kahn, O. *Molecular Magnetism*; VCH Publishers: New York, 1993. (d) *Molecule-Based Magnetic Materials: Theory, Techniques, and Applications*; Turnbull, M. M., Sugimoto, T., Thompson, L. K., Eds.; ACS Symposium Series 644; American Chemical Society: Washington, DC, 1996.

(14) A preliminary report has been presented: Monari, M.; Pandolfo, L.; Pettinari, C. 7° FIGIPS Meeting in Inorganic Chemistry, Lisbon, June 11–14, 2003; p 323.

The electrical conductances of the acetonitrile solutions were measured with a Crison CDTM 522 conductimeter at room temperature. Positive and negative electrospray mass spectra were obtained with a series 1100 MSI detector HP spectrometer, using an acetonitrile mobile phase. Solutions for electrospray ionization mass spectrometry (ESI-MS) were prepared using reagent grade acetone or acetonitrile, and the obtained data (masses and intensities) were compared to those calculated by using the IsoPro isotopic abundance simulator, version 2.1.[15] Peaks containing copper(II) ions are identified as the centers of isotopic clusters. The magnetic susceptibilities were measured at room temperature ($20-28$ °C) by the Gouy method, with a Sherwood Scientific magnetic balance, MSB-Auto, using $HgCo(NCS)_4$ as calibrant and correcting for diamagnetism with the appropriate Pascal constants. The magnetic moments (μ_B) were calculated from the equation $\mu_{eff} = 2.84(X_m^{corr}T)^{1/2}$. The EPR spectra were recorded with a Bruker ER 200 X-band spectrometer equipped with a nitrogen flow variable-temperature system. UV-vis spectra were recorded on a Varian Cary 5E spectrophotometer, equipped with a device for reflectance measurements.

Computational Details. Density functional (DF) calculations were carried out by using the ADF 2002 package.[16] Optimized geometries and vibrational parameters were evaluated by employing generalized gradient (GGA) corrections self-consistently included through the Becke-Perdew (BP) formula.[17] A triple-ζ Slater-type basis set was used for (i) Cu atoms, (ii) all the atoms directly bonded to them, and (iii) the hydroxyl and pyrazole H atoms, whereas a double-ζ basis set was adopted for the remaining atoms of the complex. The inner cores of Cu (1s2s2p), O (1s), C (1s), and N (1s) atoms were kept frozen throughout the calculations. All the numerical experiments were carried out by including spin-polarization effects. Energy differences associated with electronic transitions were evaluated by using the Slater transition-state procedure.[18] Moreover, the EPR **g** tensor was computed by employing the method proposed by van Lenthe and co-workers.[19,20] Finally, force constants and harmonic frequencies were calculated by numerical differentiation of energy gradients computed both at the equilibrium geometry and at slightly deviating geometries. Information about the localization and the bonding/antibonding character of selected molecular orbitals (MOs) over a broad range of energy was obtained by referring to the density of states (DOS), partial DOS (PDOS), and crystal orbital overlap population (COOP). Corresponding curves were computed by weighting one-electron energy levels by their basis orbital percentage and by applying a 0.25 eV Lorentzian broadening.

Catalytic Experiments. The reactions were carried out in dry chloroform that was distilled over P_2O_5 under nitrogen before use. All other reagents and solvents were of the highest analytical grade and used without further purification. Chromatographic purifications were performed on silica gel ($35-70$ mesh, Merck) columns. Thin-layer chromatography was carried out using Merck Kiesegel 60 F254 plates. GC analyses were performed on a Carlo Erba HRGC 5160 instrument equipped with a 30 m Supelco SPB-35 GC column and an FID detector.

General Procedure for the Cyclopropanation Reactions. The reactions and workup were carried out as reported in the literature.[21] The GC analyses of the products were performed under the following conditions: initial (5 min) and final temperatures of 70 and 200 °C, respectively, heating rate 10 °C min⁻¹. The chemical yields were not optimized. The obtained data were reproducible within ±2% for several experiments.

Syntheses. [Cu₃(μ₃-OH)(μ-pz)₃(MeCOO)₂(Hpz)] (1). Hpz (0.680 g, 10 mmol) and Cu(MeCOO)₂·H₂O (1.50 g, 7.5 mmol) were dissolved in 50 mL of EtOH. The solution was stirred overnight at room temperature. A blue microcrystalline precipitate formed which was filtered, washed with EtOH, dried under vacuum, and identified as compound **1** (1.35 g, 2.27 mmol, 90% yield). Acetic acid was found in mother liquors. Compound **1** was recrystallized from hot EtOH, yielding well-formed hexagonal platelets, suitable for X-ray crystal structure determination. Mp: 228 °C dec, 306 °C chars. Anal. Calcd for $C_{16}H_{20}N_8O_5Cu_3$: C, 32.30; H, 3.39; N, 18.83; O, 13.44. Found: C, 32.23; H, 3.44; N, 18.82; O, 13.30. IR (Nujol, cm⁻¹): 3250br, 3180sh, 3110m, 1576s, 1488m, 1450s, 1383s, 1351s, 1338s, 1276m, 1175m, 1156m, 1152m, 1059s, 931m, 817m, 774m, 748s, 457m, 350s, 325m. ESI MS (+) (H₂O/MeOH) (higher peaks; relative abundance, %): m/z 381 (7) [Cu₂(pz)(MeCOO)₂-(Hpz)]⁺, 468 (50) [Cu₃(OH)(pz)₃(MeCOO)]⁺, 476 (45) [Cu₃(OH)-(pz)₄]⁺, 510 (20) [Cu₃(pz)₃(MeCOO)₂]⁺ 518 (55) [Cu₃(pz)₄-(MeCOO)]⁺, 526 (15) [Cu₃(pz)₅]⁺, 550 (70) [Cu₃(pz)₄(MeCOO)-(MeOH)]⁺, 578 (100) [Cu₃(pz)₃(MeCOO)₂(Hpz)]⁺, 586 (80) [Cu₃-(pz)₄(MeCOO)(Hpz)]⁺, 600 (10) [Cu₃(pz)₄(MeCOO)₂+Na]⁺, 618 (20) [Cu₃(OH)(pz)₃(MeCOO)₂(Hpz)+Na]⁺. μ_{eff}(296 K): 2.156 μ_B. Λ_M(EtOH, 1×10^{-4} M): 1.0 Ω^{-1} mol² cm⁻¹. λ_{max}/nm(reflectance): 611, 648. λ_{max}/nm(MeOH solution): 621 ($\epsilon = 183$).

[Cu₃(μ₃-OH)(μ-pz)₃(MeCOO)(MeO)(Hpz)] (2). MeONa (0.054 g, 1 mmol) was added to a methanol solution/suspension of compound **1** (0.59 g, 1 mmol). The suspension was stirred overnight at room temperature. The pale-blue precipitate formed was filtered off, washed with EtOH/Et₂O, dried under vacuum, and identified as compound **2** (0.340 g, 0.6 mmol, 60% yield). Mp: $289-290$ °C dec. Anal. Calcd for $C_{15}H_{20}Cu_3N_8O_4$: C, 31.77; H, 3.56; N,19.76; O, 11.29. Found: C, 31.95; H, 3.65; N,19.82; O, 11.11. IR (Nujol, cm⁻¹): 3250br, 3180sh, 3117m, 3106m, 3060sh, 1578s, 1490m, 1460s, 1391s, 1378s, 1353m, 1340m, 1281m, 1176m, 1159w, 1151w, 1114w, 1071sh, 1060s, 1021w, 931m, 911w, 887w, 843w, 817w, 774m, 762s, 722m, 679s, 627m, 617m, 613m, 532m, 488w, 457m, 419w, 412w, 350s, 325w, 314w, 291w, 280w, 229m. ESI MS (+) (H₂O/MeOH) (higher peak): m/z 550 [Cu₃(MeO)(pz)₃-(MeCOO)(Hpz)]⁺. μ_{eff}(296 K): 2.15 μ_B. Λ_M(EtOH, 1×10^{-4} M): 0.4 Ω^{-1} mol² cm⁻¹.

[Cu₃(μ₃-OH)(μ-pz)₃(MeO)₂(Hpz)] (3). By reacting **1** (0.59 g, 1 mmol) with MeONa (0.170 g, 3.0 mmol) according to the same procedure employed for **2**, compound **3** was obtained (0.350 g, 0.65 mmol, 65% yield) as a blue-gray insoluble solid. Mp: $290-294$ °C dec. Anal. Calcd for $C_{14}H_{20}Cu_3N_8O_3$: C, 31.20; H, 3.74; N, 20.79; O, 8.91. Found: C, 31.10; H, 3.55; N, 21.00; O, 9.21%. IR (Nujol, cm⁻¹): 3220br, 3120w, 3104w, 1586m, 1578m, 1489m, 1463s, 1283m, 1180m, 1170w, 1061m, 921w, 868w, 747m, 679w, 668w, 630m, 618s, 531br, 366m, 280m. ESI MS (+) (H₂O/MeOH) (higher peak): m/z 522 [Cu₃(MeO)₂(pz)₃(Hpz)]⁺. μ_{eff}(296 K): 2.093 μ_B. Λ_M(EtOH, 1×10^{-4} M): 0.2 Ω^{-1} mol² cm⁻¹.

[Cu(MeCOO)₂(4-MepzH)₂(H₂O)₂] (4). 4-MepzH (1.23 g, 15 mmol) and Cu(MeCOO)₂·H₂O (1.50 g, 7.5 mmol) were dissolved in 50 mL of an 80/20 mixture of EtOH/H₂O. The solution was

(15) Senko, M. W. *IsoPro Isotopic Abundance Simulator*, v. 2.1; National High Magnetic Field Laboratory, Los Alamos National Laboratory: Los Alamos, NM.

(16) *Amsterdam Density Functional Package*, Version 2002; Vrjie Universiteit: Amsterdam, The Netherlands, 2002.

(17) (a) Becke, A. D. *Phys. Rev. A* **1988**, *38*, 3098. (b) Perdew, J. P. *Phys. Rev. B* **1986**, *33*, 8822.

(18) Slater, J. C. *Adv. Quantum Chem.* **1972**, *6*, 1.

(19) van Lenthe, E.; Baerends, E. J. *J. Chem. Phys.* **2000**, *112*, 8278.

(20) The frozen core approximation for Cu and O inner cores has been lifted during calculations pertaining to the evaluation of the **g** tensor.

(21) Simkhovich, L.; Mahammed, A.; Goldberg, I.; Gross, Z. *Chem.—Eur. J.* **2001**, *7*, 1041.

stirred overnight at room temperature and then evaporated under vacuum and the blue residue obtained washed with EtOH/Et$_2$O (1/1) (50 mL). A blue microcrystalline compound was obtained which was recrystallized from EtOH/Et$_2$O (1/2), dried under vacuum, and identified as compound **4** (1.43 g, 4.5 mmol, 60% yield). Mp: 79−82 °C. Anal. Calcd for C$_{12}$H$_{22}$N$_4$O$_6$Cu: C, 37.74; H, 5.81; N, 14.67; O, 25.14. Found: C, 38.01; H, 5.70; N, 14.68; O, 25.37. IR (Nujol, cm^{-1}): 3350br, 3215sbr, 3137sh, 3090sh, 1610s, 1586s, 1556sh, 1505m, 1456s, 1400s, 1335s, 1319sh, 1270m, 1237m, 11712m, 110s, 1077s, 1045m, 1016m, 967m, 931m, 833s, 675m, 657s, 627s, 489br, 393w, 331br. ESI MS (+) (H$_2$O/MeOH) (higher peak): m/z 286 [Cu(MeCOO)(4-MepzH)$_2$]$^+$. μ_{eff}(296 K): 1.89 μ_B. Λ_M(EtOH, 1 × 10^{-3} M): 2.0 Ω^{-1} mol^2 cm^{-1}.

[Cu(MeCOO)$_2$(3,5-Me$_2$pzH)$_2$] (5). Compound **5** was prepared by following the same procedure described for **4**, obtaining a pale blue solid (80% yield). Mp: 168 °C. Anal. Calcd for C$_{14}$H$_{22}$N$_4$O$_4$Cu: C, 44.97; H, 5.93; N,14.98; O, 17.12. Found: C, 45.01; H, 6.02; N, 14.87; O, 16.96. IR (Nujol, cm^{-1}): 3430 br, 3183m, 3110m, 3085m, 3060sh, 1557br, 1459m, 1380br, 1307s, 1185m, 1152m, 1052m, 1025m, 1012m, 986w, 937w, 830br, 742m, 722m, 684m, 675s, 637w, 622m, 473m, 428m, 348m, 313s. ESI MS (+) (H$_2$O/MeOH) (higher peak): m/z 314 [Cu(Me$_2$pzH)$_2$(MeCOO)]$^+$. μ_{eff}(296 K): 1.83 μ_B. Λ_M(EtOH, 1 × 10^{-3} M): 1.7 Ω^{-1} mol^2 cm^{-1}.

[Cu(MeCOO)$_2$(3,4,5-Me$_3$pzH)$_2$] (6). Compound **6** was prepared by following the same procedure described for **4**, obtaining a pale blue solid (76% yield). Mp: 195−197 °C. Anal. Calcd for C$_{16}$H$_{26}$N$_4$O$_4$Cu: C, 47.81; H, 6.52; N, 13.94; O, 15.92. Found: C, 47.74; H, 6.82; N, 14.01; O, 15.96. IR (Nujol, cm^{-1}): 3200−2800br, 3180br, 3134s, 3086s, 1556br, 1524br, 1341s, 1302s, 1275m, 1178s, 1025m, 1015m, 938m, 830s, 764m, 722w, 708w, 670m, 621w, 571w, 493w, 472w, 343w, 311s, 291m. ESI MS (+) (H$_2$O/MeOH) (higher peak): m/z 342 [Cu(3,4,5-Me$_3$pzH)$_2$(MeCOO)]$^+$. μ_{eff}(296 K): 1.89 μ_B. Λ_M(EtOH, 1 × 10^{-3} M): 1.2 Ω^{-1} mol^2 cm^{-1}.

[Cu(MeCOO)$_2$(3-Me-5-PhpzH)$_2$(H$_2$O)$_2$] (7). Compound **7** was prepared by following the same procedure described for **4**, obtaining a pale blue solid (80% yield). Mp: 136−137 °C. Anal. Calcd for C$_{24}$H$_{26}$CuN$_4$O$_4$: C, 57.88; H, 5.26; N, 11.25; O, 12.85. Found: C, 57.58; H, 5.39; N, 11.44; O, 12.45. IR (Nujol, cm^{-1}): 3200−2800br, 3100br sh, 1604s, 1580s br, 1560s, 1549s, 1250br, 1187m, 1155m, 1107s, 1072m, 1016m, 1006m, 992w, 967m, 909m, 762s, 721m, 696s, 618m, 539m, 524m, 421br, 280br. ESI MS (+) (H$_2$O/MeOH) (higher peak): m/z 438 [Cu(3-Me-5-PhpzH)$_2$(MeCOO)]$^+$. μ_{eff}(296 K): 2.02 μ_B. Λ_M(EtOH, 1 × 10^{-3} M): 1.2 Ω^{-1} mol^2 cm^{-1}.

[Cu(MeCOO)$_2$(3-Me-4-PhpzH)$_2$] (8). 3-Me-4-PhpzH (0.320 g, 2 mmol) was added to an ethanol solution of Cu(MeCOO)$_2$·H$_2$O (0.200 g, 1 mmol). The solution was stirred under reflux for 24 h and then evaporated under vacuum and the residue washed with an EtOH/Et$_2$O (1/1) solution (30 mL). A pale-blue precipitate formed that was identified as compound **8** (78% yield). Mp: 183−185 °C. Anal. Calcd for C$_{24}$H$_{26}$CuN$_4$O$_4$: C, 57.88; H, 5.26; N, 11.25; O, 12.85. Found: C, 57.87; H, 5.09; N, 11.39; O, 12.65. IR (Nujol, cm^{-1}): 3400br, 3189m, 3104w, 1605m, 1570s, 1530s, 1455s, 1345m, 1152m, 1104m, 1019m, 1006m, 967w, 814m, 761m, 719m, 697m, 667m, 618w, 537w, 584w, 420w, 302br. ESI MS (+) (H$_2$O/MeOH) (higher peak): m/z 438 [Cu(3-Me-4-PhpzH)$_2$(MeCOO)]$^+$. μ_{eff}(296 K): 2.00 μ_B. Λ_M(EtOH, 1 × 10^{-3} M): 2.0 Ω^{-1} mol^2 cm^{-1}.

[Cu(MeCOO)$_2$(3,4,5-Me$_3$pzH)]$_2$ (9). Compound **9** was prepared by reaction of 1 mmol of 3,4,5-Me$_3$pzH with 1 mmol of Cu-(MeCOO)$_2$·H$_2$O in refluxed ethanol (20 mL). After 24 h petroleum ether (40−60 °C) was added, and a pale green precipitate formed that was identified as compound **10** (56% yield). Anal. Calcd for

C$_{20}$H$_{32}$Cu$_2$N$_4$O$_8$: C, 41.16; H, 5.53; N, 9.60; O, 21.93. Found: C, 41.20; H, 5.81; N, 9.60; O, 22.43%. IR (Nujol, cm^{-1}): 3200s, 3156m, 3098m, 1644s, 1612s, 1586s, 1521s, 1426s, 1374s, 1341m, 1292m, 1211m, 1162m, 1120w, 1048s, 1035m, 1013m, 944w, 785w, 722m, 681s, 626m, 480w, 348s. 288m. 268m. ESI MS (+) (H$_2$O/MeOH) (higher peaks; relative abundance, %): m/z 111 (10) [Me$_3$pzH$_2$]$^+$, 282 (40) [Cu(3,4,5-Me$_3$pzH)(MeCOO)(H$_2$O)(MeOH)]$^+$, 515 (20) [Cu$_2$(3,4,5-Me$_3$pzH)(MeCOO)(3,4,5-Me$_3$pz)$_2$]$^+$, 573 (10) [Cu$_2$(3,4,5-Me$_3$pzH)$_2$(MeCOO)(3,4,5-Me$_3$pz)]$^+$. μ_{eff}(296 K): 1.498 μ_B. Λ_M(EtOH, 1 × 10^{-3} M): 0.3 Ω^{-1} mol^2 cm^{-1}.

[Cu(MeCOO)$_2$(3-Me-5-PhpzH)]$_2$ (10). Compound **10** was prepared by reaction of 1 mmol (0.15 g) of 3-Me-5-PhpzH with 1 mmol of Cu(MeCOO)$_2$·H$_2$O (0.20 g) in EtOH. The solution was refluxed overnight and then the solvent evaporated under vacuum. A pale green residue was obtained which was washed with ethanol/diethyl ether and identified as compound **10** (0.5 mmol, 50% yield). Mp: 171−177 °C. Anal. Calcd for C$_{28}$H$_{32}$Cu$_2$N$_4$O$_8$: C, 49.48; H, 4.75; N, 8.24; O, 18.83. Found: C, 49.30; H, 5.00; N, 8.15; O, 18.67%. IR (Nujol, cm^{-1}): 3200br, 1643br, 1604s, 1587sh, 1567m, 1380br, 1307s, 1185m, 1152m, 1052, 1025m, 1012m, 986w, 937m, 830br, 742m, 722m 684m, 675s, 637w, 622m, 473m, 428m, 348m, 313s. ESI MS (+) (H$_2$O/MeOH) (higher peaks; relative abundance, %): m/z 159 (10) [3-Me-5-PhpzH$_2$]$^+$, 438 (100) [Cu(3-Me-5-PhpzH)$_2$(MeCOO)]$^+$, 526 (20) [Cu$_2$(3-Me-5-PhpzH)$_2$(MeCOO)$_2$-(MeOH)$_2$ + H]$^+$, 656 (40) [Cu$_2$(3-Me-5-PhpzH)$_3$(MeCOO)$_2$ + H]$^+$. μ_{eff}(296 K): 1.521 μ_B. Λ_M(EtOH, 1 × 10^{-3} M): 0.6 Ω^{-1} mol^2 cm^{-1}.

[Cu(MeCOO)$_2$(3-Me-4-PhpzH)]$_2$ (11). Compound **11** was prepared by reaction of 1 mmol (0.153 g) of 3-Me-4-PhpzH with 1 mmol of Cu(MeCOO)$_2$·H$_2$O (0.218 g) in EtOH. The solution was refluxed overnight and then the solvent evaporated under vacuum. A pale green residue was obtained which was washed with ethanol/diethyl ether/petroleum ether (1/1/1) (40−60 °C) and identified as compound **11** (0.7 mmol, 70% yield). Mp: 172−173 °C dec. Anal. Calcd for C$_{28}$H$_{32}$Cu$_2$N$_4$O$_8$: C, 49.48; H, 4.75; N, 8.24; O, 18.83. Found: C, 49.63; H, 4.64; N, 8.30; O, 18.77%. IR (Nujol, cm^{-1}): 3400br, 3090m, 3032sh, 1622sh, 1609s, 1569s, 1498m, 1377s, 1364m, 1348m, 1237m, 1156m, 1110m, 1074w, 1045m, 1022m, 967w, 869w, 814m, 765s, 700s, 683s, 659s, 620m, 545m, 534m, 486w br, 420w br, 352m br, 260br. ESI MS (+) (H$_2$O/MeOH) (higher peaks; relative abundance, %): m/z 159 (10) [3-Me-4-PhpzH$_2$]$^+$, 438 (100) [Cu(3-Me-4-PhpzH)$_2$(MeCOO)]$^+$, 526 (20) [Cu$_2$(3-Me-4-PhpzH)$_2$(MeCOO)$_2$(MeOH)$_2$ + H]$^+$, 656 (40) [Cu$_2$(3-Me-4-PhpzH)$_3$(MeCOO)$_2$ + H]$^+$. μ_{eff}(296 K): 1.510 μ_B. Λ_M(EtOH, 1 × 10^{-3} M): 0.5 Ω^{-1} mol^2 cm^{-1}.

[Cu(CF$_3$COO)$_2$(Hpz)$_2$] (12). Compound **12** was prepared (74% yield) by following the same procedure described for **4** by using Cu(CF$_3$COO)$_2$·2H$_2$O prepared according to the literature.[22] Blue crystals suitable for X-ray analysis were obtained from slow evaporation of mother liquors. Mp: 172−176 °C. Anal. Calcd for C$_{10}$H$_8$CuF$_6$N$_4$O$_4$: C, 28.21; H, 1.89; N, 13.16; O, 15.03. Found: C, 28.43; H, 2.01; N, 12.99; O, 15.35. IR (Nujol, cm^{-1}): 3430br, 3163m, 3143m, 3060w, 1677br, 1644br, 1534m, 145m, 1446m, 1364m, 1279m, 1205s, 1133s, 1071m, 1055m, 856m, 846m, 797m, 771s, 765s, 725s, 610m, 600m, 520m, 340m. ESI MS (+) (H$_2$O/MeOH) (higher peak): m/z 312 [Cu(CF$_3$COO)(Hpz)$_2$]$^+$. μ_{eff}(296 K): 1.91 μ_B. Λ_M(EtOH, 1 × 10^{-3} M): 6.2 Ω^{-1} mol^2 cm^{-1}.

X-ray Crystallography. The X-ray intensity data for **1** and **12** were measured on a Bruker AXS SMART 2000 diffractometer, equipped with a CCD detector. Cell dimensions and the orientation matrix were initially determined from a least-squares refinement

---

(22) Martin, R. L.; Waterman, H. *J. Chem. Soc.* **1957**, 2545.

Table 1. Crystal Data and Experimental Details for **1** and **12**

	1	12
empirical formula	C$_{16}$H$_{20}$Cu$_3$N$_8$O$_5$	C$_{10}$H$_8$CuF$_6$N$_4$O$_4$
fw	595.02	425.74
T, K	298(2)	298(2)
λ, Å	0.71073	0.71073
cryst symmetry	monoclinic	monoclinic
space group	$P2_1/c$	Cc
a, Å	11.6602(4)	13.981(2)
b, Å	19.9062(6)	13.046(2)
c, Å	9.6896(3)	8.854(1)
β, deg	99.576(1)	94.568(3)
cell vol, Å^3	2217.7(1)	1609.8(3)
Z	4	4
D_c, Mg m^{-3}	1.782	1.757
μ(Mo Kα), mm^{-1}	2.896	1.445
$F(000)$	1196	844
cryst size, mm	0.12 × 0.20 × 0.25	0.20 × 0.25 × 0.30
θ limits, deg	1.77–30.03	2.14–30.24
no. of reflns collected	29310 (±h, ±k, ±l)	10276 (±h, ±k, ±l)
no. of unique obsd reflns [$F_o > 4\sigma(F_o)$]	6493 [R(int) = 0.092]	4689 [R(int) = 0.093]
GOF on F^2	0.969	1.041
R1(F),^{a} wR2(F^2)^b	0.0471, 0.1089	0.0562, 0.1511

^{a} R1 = $\sum||F_o| - |F_c|/\sum|F_o|$. ^{b} wR2 = $[\sum w(F_o^2 - F_c^2)^2/\sum w(F_o^2)^2]^{1/2}$. $w = 1/[\sigma^2(F_o^2) + (aP)^2 + bP]$, where $P = (F_o^2 + 2F_c^2)/3$.

on reflections measured in three sets of 20 exposures, collected in three different ω regions, and eventually refined against all data. For all crystals, a full sphere of reciprocal space was scanned by 0.3° ω steps, with the detector kept 5.0 cm from the sample. The software SMART[23] was used for collecting frames of data, indexing reflections, and determination of lattice parameters. The collected frames were then processed for integration by the SAINT program,[23] and an empirical absorption correction was applied using SAD-ABS.[24] The structures were solved by direct methods (SIR 97)[25] and subsequent Fourier syntheses and refined by full-matrix least squares on F^2 (SHELXTL),[26] using anisotropic thermal parameters for all non-hydrogen atoms. In **12**, some disorder was detected for the fluorine atoms of the trifluoroacetate groups, which were refined over two sites, yielding occupation factors of 0.67 and 0.90 for the main images of the F atoms bound to C(8) and C(10), respectively. All hydrogen atoms, except the pyrazole and hydroxy hydrogens, which were located in the Fourier map and refined isotropically, were added in calculated positions, included in the final stage of refinement with isotropic thermal parameters, U(H) = 1.2U_{eq}(C) [U(H) = 1.5U_{eq}(C-Me)], and allowed to ride on their carrier carbons. For **12** the absolute configuration was determined (Flack parameter $-0.00(2)$). Crystal data and details of the data collection for both structures are reported in Table 1.

Results and Discussion

Compound **1** [Cu$_3$(μ_3-OH)(μ-pz)$_3$(MeCOO)$_2$(Hpz)] has been obtained as a dark-blue microcrystalline solid by adding Hpz to hydrated copper(II) acetate in ethanol at room temperature (Scheme 1) without addition of hydroxide ions

(23) *SMART & SAINT Software Reference Manuals*, version 5.051 (Windows NT Version); Bruker Analytical X-ray Instruments Inc.: Madison, WI, 1998.
(24) Sheldrick, G. M. *SADABS, program for empirical absorption correction*; University of Göttingen: Göttingen, Germany, 1996.
(25) Altomare, A.; Cascarano, G.; Giacovazzo, C.; Guagliardi, A.; Moliterni, A. G. G.; Burla, M. C.; Polidori, G.; Camalli, M.; Siliqi, D. *Acta Crystallogr., Sect. A* **1996**, *52*, C79.
(26) Sheldrick, G. M. *SHELXTLplus (Windows NT Version) Structure Determination Package*, Version 5.1; Bruker Analytical X-ray Instruments Inc.: Madison, WI, 1998.
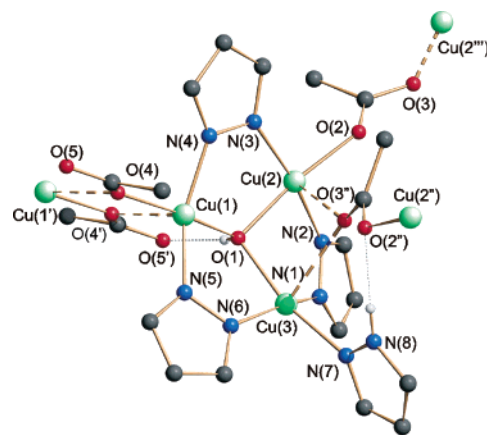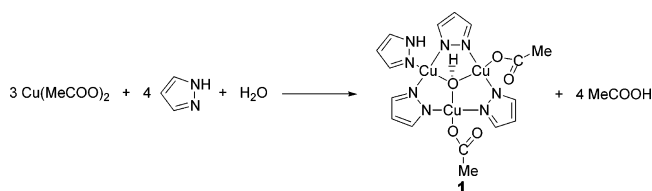
Figure 1. Molecular structure of **1** showing O–H···O and N–H···O interactions (dotted lines). Dashed lines indicate the weaker Cu–O bonds in the coordination sphere of Cu(1), Cu(2), and Cu(3). Symmetry code: (I) $-x$, $-y$, $-z$; (II) x, $-y + 0.5$, $z + 0.5$; (III) x, $-y + 0.5$, $z - 0.5$. Hydrogen atoms not involved in hydrogen bonding have been omitted for clarity.

Scheme 1

or other bases.[27] The same compound was obtained also by carrying out the reaction in H$_2$O or in non-hydroalcoholic media, such as diethyl ether, light petroleum ether, or acetonitrile. As an example, in water the reaction is almost immediate, and solid **1** precipitates after 2 or 3 min and can be recrystallized from EtOH, yielding well-formed deep-blue crystals. A 4:3 Hpz:Cu ratio is not strictly required; however, it provides the higher yield.

Compound **1** is poorly soluble in alcohols, very slightly soluble in water, and almost insoluble in hydrocarbons, chlorinated solvents, acetone, and acetonitrile. It was characterized through elemental analysis, IR and UV–vis spectra, ESI MS, room temperature magnetic susceptibility measurements, and X-ray crystal structure determination. Particularly, a positive ESI mass spectrum of a methanol/water solution shows the most intense signal as a cluster centered at m/z 578, exactly simulated by [Cu$_3$pz$_3$(MeCOO)$_2$(Hpz)]$^+$, and a signal centered at m/z 618 (20% relative abundance) corresponds to [**1** + Na]$^+$. Moreover, all other relevant signals show patterns typical for ions containing a Cu$_3$ system.

The X-ray molecular structure of **1** (Figure 1) reveals several interesting features. Complex **1** is made of a trinuclear [Cu$_3$(μ_3-OH)(μ-pz)$_3$]$^{2+}$ core in which the copper ions, held together by the trihapto oxygen of the hydroxy group and three bridging pyrazolate ligands, lie at the corners of an irregular triangle. The charge balance is completed by two acetate ions bonded to Cu(1) and Cu(2), whereas a neutral pyrazole is bonded to Cu(3). The coordination geometry at Cu(1), Cu(2), and Cu(3) is square pyramidal[28] with the apical

(27) If exogenous bases, such as NaOH, are added to the reaction pot, brown uncharacterized material(s) form.

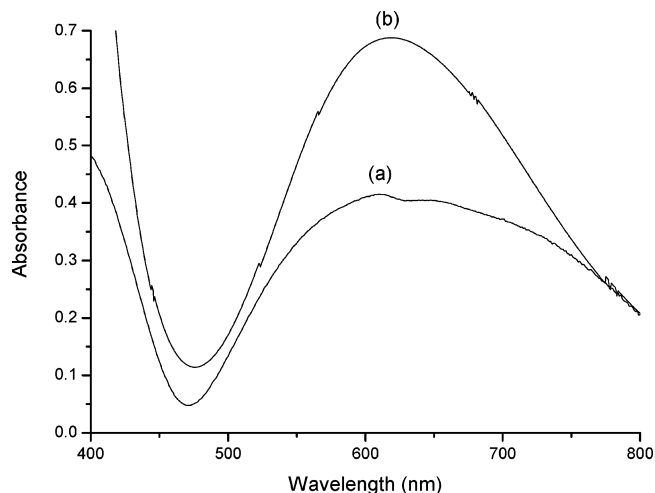**Table 2.** Selected Bond Lengths (Å) and Angles (deg) for **1**

Cu(1)−O(1)	1.953(2)	Cu(2)−N(3)	1.959(3)	Cu(1)−O(4)	1.966(2)
Cu(2)−O(1)	1.978(2)	Cu(3)−N(1)	1.965(3)	Cu(1)−O(4′)^a	2.377(3)
Cu(3)−O(1)	1.969(3)	Cu(3)−N(6)	1.956(3)	Cu(3)−N(7)	2.001(4)
Cu(1)−N(4)	1.962(3)	Cu(3)−N(7)	2.001(4)	Cu(1)···Cu(2)	3.3697(6)
Cu(1)−N(5)	1.949(3)	Cu(2)−O(2)	1.965(3)	Cu(2)···Cu(3)	3.0818(6)
Cu(2)−N(2)	1.976(3)	Cu(2)−O(3″)^a	2.280(3)	Cu(1)···Cu(3)	3.3173(7)
Cu(1)−O(1)−Cu(2)	118.0(1)	N(4)−Cu(1)−N(5)	156.8(2)	O(1)−Cu(1)−O(4)	168.4(1)
Cu(1)−O(1)−Cu(3)	115.5(1)	N(2)−Cu(2)−N(3)	168.7(1)	O(1)−Cu(2)−O(2)	172.0(1)
Cu(2)−O(1)−Cu(3)	102.7(1)	N(1)−Cu(3)−N(6)	158.4(1)	O(1)−Cu(3)−N(7)	164.6(1)

^{a} Symmetry code: (I) −x, −y, −z; (II) x, −y + 0.5, z − 0.5.
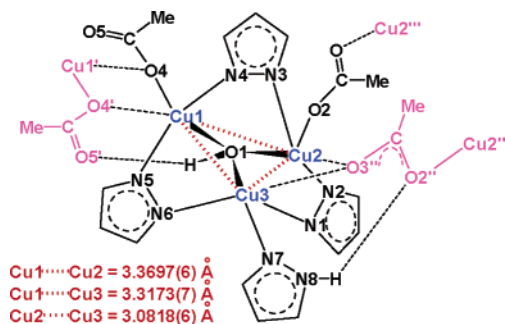
Figure 2. Partial sketch of the intermolecular interactions among four trinuclear triangular units of **1**.

Figure 3. Solid-state (a) and MeOH solution (b) electronic spectra of **1**.

positions occupied by an oxygen of an acetate ligand. The distances between the three copper ions and μ_3-OH are similar [Cu(1)−O(1) = 1.953(2) Å, Cu(2)−O(1) = 1.978(2) Å, Cu(3)−O(1) = 1.969(3) Å, Cu−O(H)$_{av}$ = 1.967(5) Å] (see Table 2 for bond lengths and angles of **1**) and shorter than those reported for the other complexes containing the [Cu$_3$(μ_3-OH)(μ-pz)$_3$]$^{2+}$ system.[2d,7] Interestingly, in **1** two of the Cu−O(H)−Cu angles [Cu(1)−O(1)−Cu(3) and Cu(1)−O(1)−Cu(2) = 115.5(1)° and 118.0(1)°, respectively] are very close to each other but quite different from the third one [Cu(2)−O(1)−Cu(3) = 102.6(1)°], and as a consequence, the nonbonding copper−copper distances Cu(1)···Cu(3) and Cu(1)···Cu(2) are similar whereas the Cu(2)···Cu(3) separation is the shortest one (see Figure 2). The capping μ_3-O(1)H is displaced about 0.563(2) Å out of the Cu$_3$ plane, and forms with the three copper ions a very flat tetrahedron. The two pyrazolate rings bearing N(3)−N(4) and N(5)−N(6) are almost coplanar with the Cu$_3$ plane, whereas the third one [(N(1)−N(2)] is displaced out of the Cu$_3$ plane on the same side of the hydroxy group to alleviate the steric hindrance of the neutral pyrazole coordinated to Cu(3). The Cu−N(bridged) distances fall in the range 1.949(3)−1.976(3) Å.

Each trinuclear triangular unit [Cu$_3$(μ_3-OH)(μ-pz)$_3$(Me-COO)$_2$(Hpz)] interacts in an asymmetric fashion with other three, forming a "polymeric" bidimensional network partially sketched in Figure 2. Both Cu(1) and Cu(2) show an almost regular square pyramidal geometry with the more weakly bound acetate oxygen atom in the axial position, but the arrangements of the acetate ligands around the metals are different. In fact, the coordination at Cu(1) is achieved by

(28) τ parameter values 0.19, 0.05, and 0.11 for Cu(1), Cu(2), and Cu(3), respectively, according to Addison, A. W.; Rao, T. N.; Redijk, J.; van Rijn, J.; Verschoor, G. C. *J. Chem. Soc., Dalton Trans.* **1984**, 1349.

two oxygens of different acetates doubly bridging in an asymmetric mode two copper ions belonging to distinct trinuclear units [Cu(1)−O(4) = 1.966(2) Å, Cu(1)−O(4′) = 2.377(3) Å], whereas the acetate ligands bound at Cu(2) use for the coordination to the metals both oxygens, one for the stronger interaction [Cu(2)−O(2) = 1.965(3) Å] and one for the weaker interaction [Cu(2)−O(3″) = 2.280(3)]. In addition, the acetate oxygen [O(3″)] involved in the coordination to Cu(2) bridges the shortest Cu(2)···Cu(3) separation, establishing an additional weak interaction with Cu(3) [Cu(3)−O(3″) = 2.485(3) Å] that has an irregular square pyramidal geometry. Further stabilization of the solid-state network arises from intermolecular hydrogen bonds between the H atom of the μ_3-OH group and the acetate oxygen O(5′) [O(1)···O(5′) = 2.677(4) Å, O(1)−H−O(5′) = 164(4)°] and the N−H proton of the pyrazole and the acetate oxygen O(2″) [N(8)···O(2″) = 2.828(5)°, N(8)−H(81)−O(2″) = 177(5)°]. Interestingly, the intermolecular Cu(1)···Cu(1′) distance, bridged by two acetate ligands, is very short [3.3355(9) Å].

The low solubility of **1** hampered any attempt to perform electrochemical experiments on it, whereas it was possible to record its MeOH solution electronic spectrum. Solution and solid-state reflectance spectra in the range 400−800 nm are reported in Figure 3. The reflectance electronic spectrum of **1** (Figure 3a) displays a complex absorption band in the range 600−700 nm, in which two maxima at 611 and 648 nm (2.03 and 1.91 eV, respectively) and a shoulder at ∼720 nm (1.72 eV) are present. The spectral pattern remains practically unchanged in solution (methanol and water). Particularly, the spectrum in MeOH solution (Figure 3b)
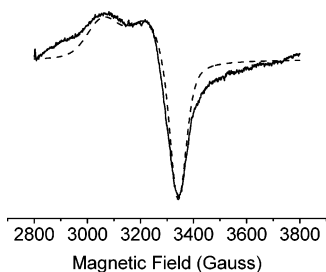
Figure 4. EPR spectrum of a polycrystalline powder sample of **1**: experimental spectrum (solid line) recorded at $T = 120$ K and simulated spectrum (dashed line). The simulation has been carried out assuming an $S = 1/2$ species with the g principal values and line width reported in the text.

shows a mediated broad, asymmetric signal centered at 621 nm ($\epsilon = 183$).

The room temperature EPR powder spectrum of **1** consists of a very broad (200 G) asymmetric line with no structure. By lowering the temperature, the line width decreases and the spectrum recorded at 120 K (see Figure 4) shows the typical features of a spin $S = 1/2$ species with an anisotropic g factor. The best computer simulation is obtained by using the following parameters: $g_{xx} = 2.015$, $g_{yy} = 2.050$, $g_{zz} = 2.200$. Since no hyperfine structure is observed, the hyperfine interaction was considered as a contribution to the line width: $\Delta B_x = 50$ G, $\Delta B_y = \Delta B_z = 110$ G. On the other hand, a proper consideration of this interaction should in principle take into account three Cu nuclei with different hyperfine couplings and the simultaneous presence of the two isotopes ^{63}Cu and ^{65}Cu, in comparable natural abundance.

The simulated spectrum is also shown in Figure 4. Even though part of the signal intensity at the spectrum wings is not reproduced, the agreement could be considered as satisfactory. The calculated ADF g components (see below) agree semiquantitatively with the experimental values.

As a whole, the above results indicate that the ground state of **1** is a doublet state. The deviation of the calculated spectrum from the experimental one and the high-temperature broadening could be assigned to the contribution of a thermally populated quartet state. The same explanation was suggested to account for the EPR features of a similar trinuclear copper complex.[29]

It is interesting to note that the g factor components are similar to those measured recently at low temperature for a spin-frustrated symmetric trinuclear copper complex, which clearly display the features of the quartet state at high temperature. For the latter derivative, also the hyperfine structure by a single Cu nucleus could be resolved, showing that the unpaired spin is localized on a single copper moiety.[30]

The X-ray crystal structure determination evidences the complete unsymmetry of **1**. The differences in the coordination environments of the three pentacoordinate copper ions likely may produce potentially interesting differences in their

electronic structures. As a matter of fact, Cu(3) beside μ_3-OH and bridging pyrazolate ligands, is coordinated to a neutral Hpz, so that its charge should be different with respect to that of Cu(1) and Cu(2) bonded to negatively charged acetate ligands. These features could have consequences on the electronic transmission among copper ions and on the magnetic behavior of compound **1**, which presents a $\mu_{eff} = 2.156 \, \mu_B$ at 296 K, a low value with respect to that expected for three independent copper(II) ions, likely an index of exchange coupling among the three metal ions.

Further insights into the electronic structure of **1** have been gained by carrying out a series of numerical experiments within the DF theory. In this regard, it can be useful to remember that each $[Cu_3(\mu_3\text{-OH})(\mu\text{-pz})_3(MeCOO)_2(Hpz)]$ molecule interacts with three other trinuclear units, two of them involving μ_3-O−H···acetate and N−H···acetate hydrogen bonding. Despite a theoretical investigation of the whole four-unit structure being out of our computational resources, the presence of the acetate groups coordinated via hydrogen bonding has been mimicked by replacing them with two molecules of acetic acid.[31] The atoms of these two molecules have been placed in the same crystallographic positions occupied by noncovalently bonded acetate ligands. Interestingly, the computed values of μ_3-O−H and N−H stretching frequencies[32] are significantly different on passing from the model without acetic acid molecules (3529 and 3595 cm^{-1}, respectively) to the one including them (3068 and 3398 cm^{-1}, respectively). The agreement with IR data (see the Experimental Section) is definitely better in the latter case, making us quite confident about the adopted model.

Now, despite the leading role in determining the stability of trinuclear units of **1** being certainly played by bridging pyrazolate ligands, their spectroscopic and magnetic properties are mostly determined by the Cu$_3(\mu_3$-OH) core.[33] A first, qualitative description of the bonding scheme of this core, simply based on symmetry arguments, can be obtained by using a well-trained method, i.e., the interacting fragment approach, which consists of dividing the whole molecules into interacting fragments and allowing the interaction of their outermost MOs. In this regard, it has already been pointed out (see the X-ray structure description) that the coordination about Cu centers is roughly square pyramidal, and it is well-known[34] that such an arrangement lifts the 5-fold degeneracy of the d orbitals to give rise to four (b$_2$ + e + a$_1$) low-lying MOs and to a partially filled b$_1$ level. The assembly of three Cu(II) centers sharing the μ_3-OH ligand will generate 30 (3 × 5 × 2) Cu-based spin orbitals (SOs), 27 of them being occupied. Cu-based SOs can be usefully divided into two sets, hereafter indicated as α and β: the former includes the linear combinations of (b$_2$ + e + a$_1$) MOs (24 low-lying SOs), and the latter is constituted by the linear combinations of the b$_1$-like level (6 high-lying SOs, 3

(29) López-Sandoval, H.; Contreras, R.; Escuer, A.; Vicente, R.; Bernès, S.; Nöth, H.; Leigh, G. J.; Barba-Behrens, N. *J. Chem. Soc., Dalton Trans.* **2002**, 2648.

(30) Cage, B.; Cotton, F. A.; Dalal, N. S.; Hillard, E. A.; Rakvin, B.; Ramsey, C. M. *J. Am. Chem. Soc.* **2003**, *125*, 5270.

(31) The hydrogen atoms of the COOH groups have been placed at 0.99 Å along the original O−Cu directions.

(32) O−H and N−H bond lengths have been optimized.

(33) (a) La Monica, G.; Ardizzoia, G. A. *Prog. Inorg. Chem.* **1997**, *46*, 151. (b) Boca, R.; Dlhá, L.; Mezei, G.; Ortiz-Pérez, T.; Raptis, R. G.; Telser, J. *Inorg. Chem.* **2003**, *42*, 5801.

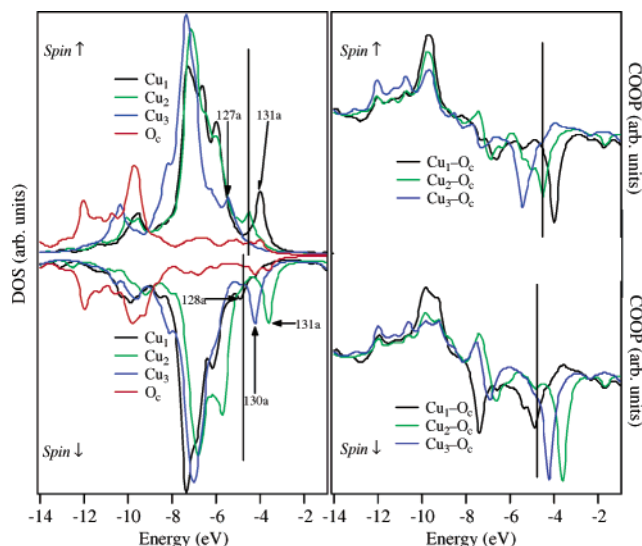(34) Rossi, A. R.; Hoffmann, R. *Inorg. Chem.* **1975**, *14*, 365.

Figure 5. Spin ↑ and spin ↓ components of the $Cu_3(\mu_3\text{-OH})$ PDOS (left) and Cu−O COOPs (right) of **1**.

of them occupied). In the presence of a local C_3 axis, the β set spans the (a + e) representations, thus having the correct symmetry to interact with the occupied (a + e) OH^- frontier orbitals.

Moving to ADF results, quantum mechanical calculations were performed for the $S = 1/2$ and $S = 3/2$ states, and in agreement with magnetic and EPR measurements, the $S = 1/2$ state was found more stable by ∼4 kcal/mol than the $S = 3/2$ one. The forthcoming discussion will then be limited to the results obtained within the assumption of a single unpaired electron. In Figure 5 the spin ↑ and the spin ↓

components of the $Cu_3(\mu_3\text{-OH})$ PDOS/COOP are reported. The inspection of the figure clearly testifies that the qualitative bonding scheme described above nicely matches ADF results. In particular, the 127a SO (↑), the 130a highest occupied SO (↑), and the 131a lowest unoccupied SO (↑) correspond to the spin ↑ component of the (a + e) β set (the spin ↓ components are the occupied 128a SO and the empty 130a and 131a SOs). It is noteworty that all these levels are Cu−OH antibonding in nature (see Figures 5 and 6) so that the $Cu_3(\mu_3\text{-OH})$ bonding scheme is characterized by the absence of any "σ" interactions (both bonding and antibonding components are occupied). At variance to that, among the SOs accounting for the $Cu_3(\mu_3\text{-OH})$ antibonding interaction of "π" symmetry [130a(↑), 131a(↑), 130a(↓), and 131a(↓)], only the first one is occupied,[35] thus implying a Cu−OH bond order of 1/2.

The proposed bonding scheme is of great value to provide a detailed assignment of the UV−vis absorption spectrum. In Figure 7 the results of Slater transition-state calculations (ΔE^{TS})[36] for spin-allowed, Cu-based excitations are reported. The agreement between theory and experiment is very good. In particular, the shoulder at 1.72 eV in the UV−vis spectrum of **1** is assigned to excitations involving SOs belonging to the β set (ΔE^{TS} values corresponding to the excitations 127a(↑) → 131a(↑) and 128a(↓) → 130a(↓) amount to 1.66 and 1.60 eV, respectively), while absorptions at 1.91 and 2.03 eV should involve the transfer of an electron from SOs belonging to the top of the α set to the lowest unoccupied SO of the β set (ΔE^{TS} values corresponding to the excitations 124a(↓) → 130a(↓) and 125a(↓) → 130a(↓) amount to 1.74 and 1.86 eV, respectively).

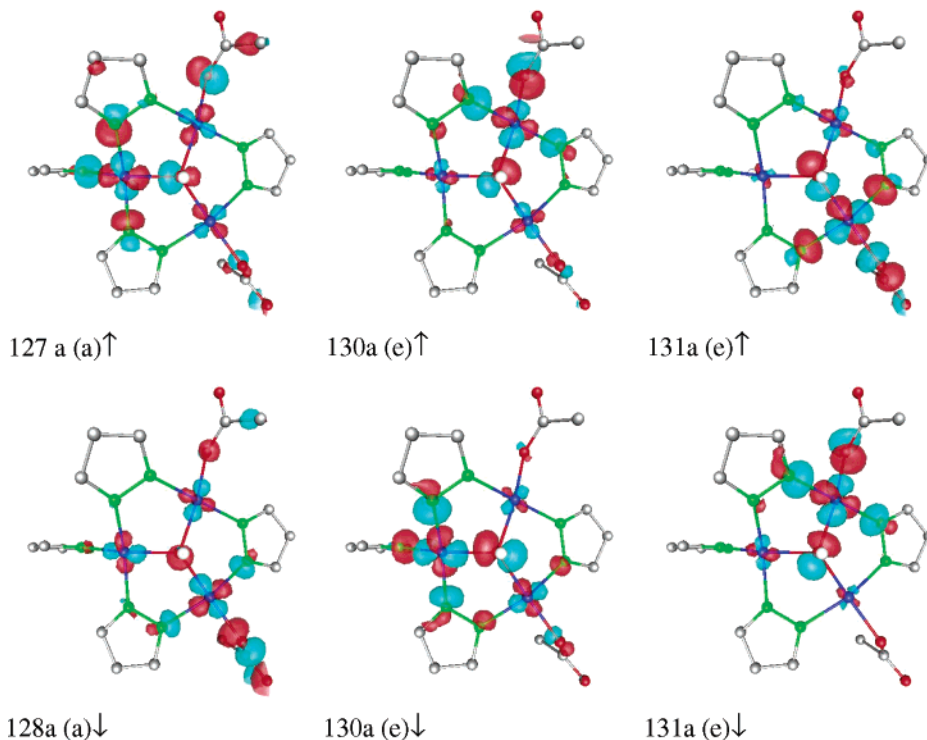**Figure 6.** 3D contour plots of the spin ↑ and spin ↓ components of the MOs belonging to the β set of **1**. Red (light blue) surfaces correspond to the positive (negative) value of 0.05 (−0.05) $e^{1/2}\ Å^{-3/2}$.
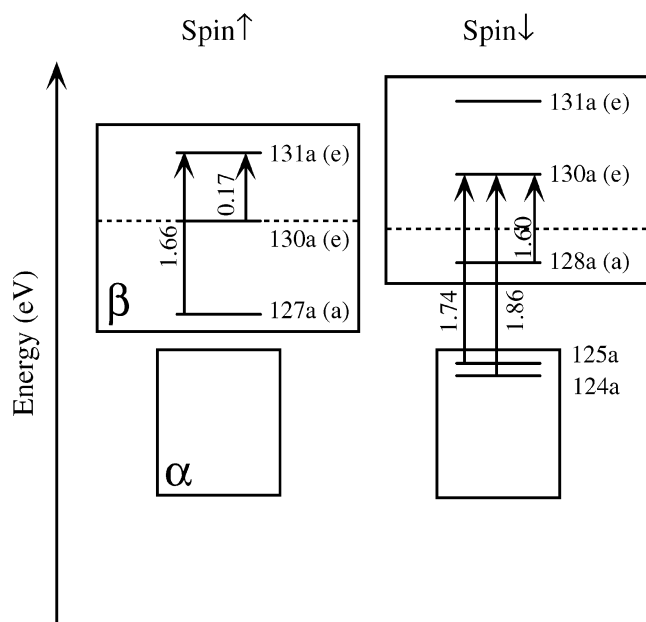
Figure 7. Qualitative outline of the frontier energy levels corresponding to the spin ↑ and spin ↓ components of the $Cu_3(\mu_3\text{-OH})$ core. Parents of the (a + e) levels are indicated in parentheses.

Components of the *g* factor for the state corresponding to $S = 1/2$ have also been computed, giving $g_{xx} = 2.042$, $g_{yy} = 2.058$, and $g_{zz} = 2.097$ values. As already mentioned they reproduce semiquantitatively EPR measurements, providing further confirmation of the suitability of the model adopted to mimic **1**. Discrepancies between theoretical and experimental values of the *g* components have to be associated with the spin contamination of our calculations, a consequence of the use of a single-determinant wave function.

As a final consideration, it is noteworthy that, in contrast to our qualitative prediction, the effective charge of Cu(3) [0.39/0.71][37] is substantially the same as that of Cu(1) [0.41/0.71] and Cu(2) [0.41/0.70], thus indicating the presence of an effective redistribution charge mechanism most likely involving bridging ligands.

Compound **1** has been reacted with a typical nucleophilic reagent, MeONa, observing the substitution of one and/or two MeCOO⁻ anions with MeO⁻, which leads to the formation of compounds [Cu₃(μ₃-OH)(μ-pz)₃(MeCOO)-(MeO)(Hpz)] (**2**) and [Cu₃(μ₃-OH)(μ-pz)₃(MeO)₂(Hpz)] (**3**), respectively, according to Scheme 2.

Compounds **2** and **3** have been characterized through elemental analysis, IR spectroscopy, ESI MS, room temperature magnetic susceptibility measurements, and positive ESI mass spectrometry (see the Experimental Section). All data are in agreement with the proposed structures. Particularly, μ_{eff} values of **2** and **3** at 296 K are 2.15 and 2.093 μ_B, respectively. The IR spectra of **2** and **3** show the presence of a broad band, typical of a OH stretching, analogous to

that found in **1**, and in addition in the IR spectrum of **3** the absorptions diagnostic for the acetate groups are absent. In the ESI MS spectra of both derivatives some peaks with a pattern characteristic of a Cu₃ cluster are always present.

As far as the formation of **1** is concerned, it is evident that it is strictly dependent on the deprotonation of H₂O and Hpz to form OH⁻ and pz⁻ ions. The acetate ion is a base strong enough to deprotonate water and Hpz, but this fact seems to be insufficient to explain the reaction course. As a matter of fact, experiments carried out in the same conditions with other azoles show a completely different reaction pattern. Actually, by reacting Cu(MeCOO)₂·H₂O with substituted pyrazoles, namely, 4-MepzH, 3,5-Me₂pzH, 3,4,5-Me₃pzH, 3-Me-4-PhpzH, and 3-Me-5PhpzH, no traces of acetic acid were detected in mother liquors and the azoles coordinate as neutral units to Cu(II), forming mononuclear species, [Cu(MeCOO)₂(4-MepzH)₂(H₂O)₂] (**4**), [Cu(MeCOO)₂(3,5-Me₂pzH)₂] (**5**), [Cu(MeCOO)₂(3,4,5-Me₃pzH)₂] (**6**), [Cu(MeCOO)₂(3-Me-5-PhpzH)₂(H₂O)₂] (**7**), and [Cu(MeCOO)₂(3-Me-4-PhpzH)₂] (**8**), always showing a 2:1 ligand to metal molar ratio. The positive ESI mass spectra of methanol/water solutions of compounds **4**−**8** show the most intense signals as clusters exactly simulated by [Cu(pzˣH)₂(MeCOO)]⁺ (pzˣH = substituted pyrazole), and also signals due to the protonated complexes [Cu(pzˣH)₂(MeCOO)₂ + H]⁺ are present. The magnetic susceptibilities data for all compounds are in the range expected for paramagnetic mononuclear Cuᴵᴵ species.

It is worth noting that when the reaction between Cu(MeCOO)₂·H₂O and some substituted pyrazole was carried out in a 1:1 ligand to metal molar ratio, the pale-green adducts **9**−**11** were obtained. On the basis of the susceptibility measurements and ESI MS and infrared data, a dimeric structure is proposed for these compounds. The μ_{eff} values are in the range expected for dimeric compounds showing antiferromagnetic coupling.[38]

Trinuclear triangular copper(II) compounds having, analogously to **1**, the [Cu₃(μ₃-OH)(μ-pz)₃] core have been previously obtained through the oxidation of suitable copper(I) complexes[7a,b] or thanks to the addition of an exogenous base to generate OH⁻ and pyrazolate ions, when CuCl₂[2d] or Cu(NO₃)₂[7c] are employed. These data point out that also the role of the anion is of paramount importance in the self-assembly of such trinuclear triangular derivatives. For this reason we have started to test the influence of the anion in the reaction course by treating, in the same conditions as for the synthesis of **1**, copper(II) trifluoroacetate with pyrazole. The formation of the mononuclear species [Cu(CF₃COO)₂(Hpz)₂] (**12**) according to Scheme 3 was observed. Compound **12** was characterized through elemental analysis, IR spectroscopy, ESI MS, room temperature magnetic susceptibility measurements and X-ray crystal structure determination.

The positive ESI mass spectrum of a methanol/water solution of compound **12** shows the most intense signal as a

(35) Occupied bonding partners are the OH⁻-based (a + e) SOs.

(36) Slater, J. C. *Quantum Theory of Molecules and Solids. Vol 4. The self-consistent-field for molecules and solids*; McGraw-Hill: New York, 1974.
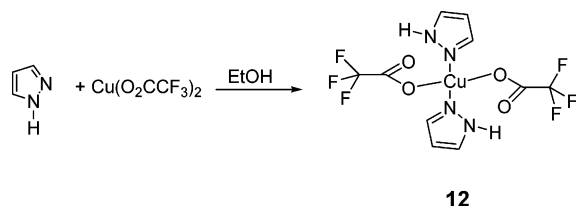
(37) The former and latter values refer to the Hirshfeld and Mulliken charge density analyses, respectively.

(38) Escrivà, E.; Garcia-Lozano, J.; Martinez-Lillo, J.; Nuñez, H.; Server-Carrió, J.; Soto, L.; Carrasco, R.; Cano, J. *Inorg. Chem.* **2003**, *42*, 8328.

Scheme 2

1 + MeONa → **2** + NaAc + MeONa → **3** + NaAc

Scheme 3

12
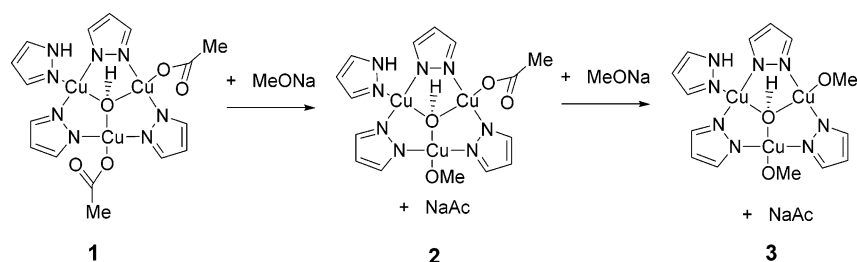
cluster exactly simulated by $[Cu(pzH)_2(CF_3COO)]^+$. The magnetic susceptibility ($\mu_{eff} = 1.91\ \mu_B$) is in the range expected for a paramagnetic mononuclear Cu^{II} species.

As far as the IR spectrum of **12** is concerned, it is generally accepted[39] that in the case of carboxylate derivatives it is possible to distinguish among ionic, unidentate, chelating bidentate, and bridging bidentate groups on the basis of Δ values [where $\Delta = \nu_a(COO) - \nu_s(COO)$], according to the generally accepted trend

$$\Delta_{unidentate} > \Delta_{ionic} > \Delta_{bridging\ bidentate} > \Delta_{chelating\ bidentate}$$

In compound **12** the Δ value is ca. 30 cm^{-1}, indicating a bridging bidentate coordination, a feature confirmed also by the X-ray molecular structure determination.

The molecular structure of **12** is shown in Figure 8, and relevant bond lengths and angles are reported in Table 3. The copper atom has a distorted square pyramidal surrounding with two trifluoroacetate groups in *trans* positions coordinated to the metal center in a monodentate fashion through the oxygen atoms and two pyrazole N atoms occupying the basal sites. The apical position is occupied by one oxygen of a trifluoroacetate group belonging to another molecule [Cu−O(4″) = 2.279(3) Å]. The two CF_3COO^- groups are nonequivalent because of their different intermolecular interactions. In fact the two oxygens of one CF_3COO^- ligand occupy one basal and one apical vertex, respectively, of a square pyramid, whereas one oxygen of the second CF_3COO^- group establishes an intermolecular hydrogen bond with one pyrazole [N(4)···O(2) = 2.88 Å, N−H···O = 155.3°]. The two pyrazole rings are tilted with respect to each other [dihedral angle 50.9(5)°] presumably to optimize the aforementioned hydrogen bond in which one of the two rings is engaged. The Cu−O distances [Cu−O(1) = 1.959 Å, Cu−O(3) 1.999(3) Å] are shorter than those found in the square bipyramidal $Cu(CF_3COO)_2(4\text{-}Mepz)_4$ [Cu−O = 2.452(3) Å][40] and slightly longer than those found, for

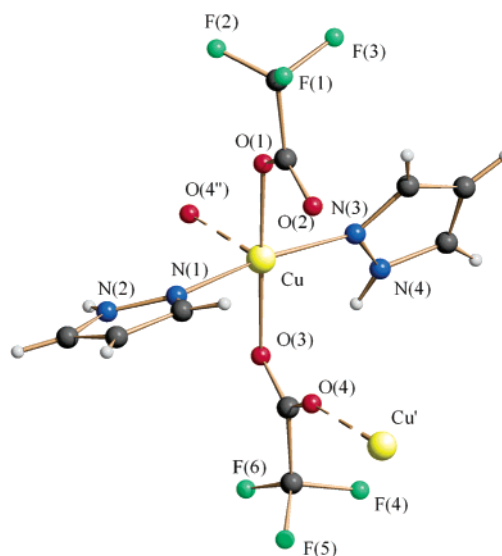**Figure 8.** Molecular structure of **12** showing the intermolecular Cu−O interactions with two neighboring molecules. Symmetry code: (I) x, $-y$, $z + 0.5$; (II) x, $-y$, $z - 0.5$.

example, in $Cu(CF_3COO)_2(IMPh)_4$ (IMPh = 2-phenyl-4,4,5,5-tetramethyl-4,5-dihydro-1*H*-imidazolin-1-oxyl) [Cu−O = 1.948(4) Å].[41] In the solid-state complex **12** is polymeric and forms infinite zigzag chains (Figure 9).

The formation of the mononuclear compound **12** instead of a trinuclear one clearly points out the relevance of the strength of the anion in determining the course of the reaction. As a matter of fact, CF_3COO^- has a steric hindrance, toward the coordination site, very similar to that of CH_3COO^-, but trifluoroacetic acid is stronger than acetic acid. For this reason, the weaker base CF_3COO^- is unable to deprotonate H_2O and Hpz to form OH^- and pz$^-$ ions, in the same extent that CH_3COO^- does. It is likely that a suitable addition of NaOH to the synthesis pot should be able to form the above-indicated ions, thus leading to the formation of a trinuclear triangular species, similar to **1**, as was observed in some other cases.[2d,7c]

Catalytic Experiments

The cyclopropyl ring formation is an important reaction in organic synthesis due to the presence of such a structure in a number of interesting natural products. Many methods have been developed in the past to achieve such reaction, and several copper, rhodium, and osmium complexes have been reported to be efficient catalysts for the cyclopropa-

(39) Deacon, G. B.; Phillips, R. J. *Coord. Chem. Rev.* **1980**, *33*, 227.
(40) Kogane, T.; Harada, K.; Umehara, M.; Hirota, R.; Nakahara, M. *Bull. Chem. Soc. Jpn.* **1992**, *65*, 2638.
(41) Cogne, A.; Laugier, J.; Luneau, D.; Rey, P. *Inorg. Chem.* **2000**, *39*, 5510.

Table 3. Selected Bond Lengths (Å) and Angles (deg) for **12**

Cu−O(1)	1.959(3)	Cu−N(3)	1.974(5)	Cu−O(4″)^a	2.279(3)
Cu−N(1)	1.994(4)	Cu−O(3)	1.999(3)		
N(1)−Cu−N(3)	170.1(2)	O(1)−Cu−N(1)	92.1(2)	N(3)−Cu−O(1)	90.5(2)
O(1)−Cu−O(3)	178.8(2)	O(3)−Cu−N(3)	88.3(2)		

^{a} Symmetry code: (II) x, $-y$, $z - 0.5$.
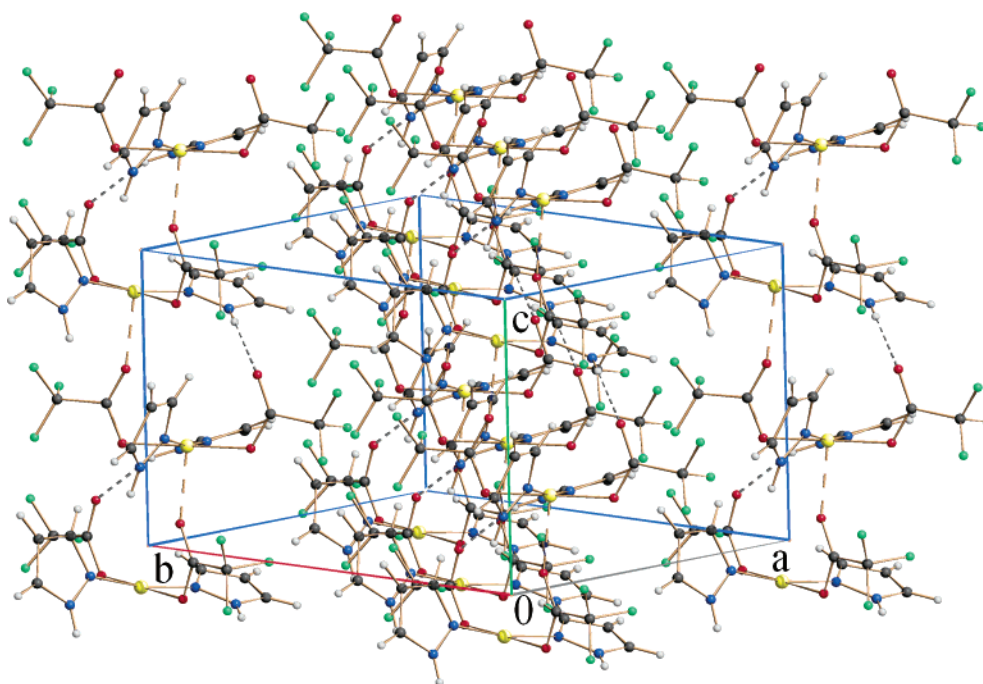
Figure 9. Crystal packing of **12** showing the polymeric zigzag chains running along the *c* axis.

Scheme 4
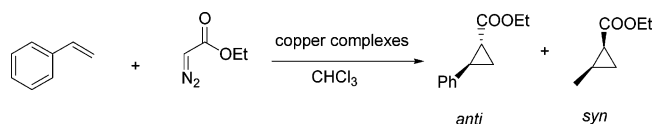
nation of olefins by diazo compounds.[42,43] Among the transition-metal reagents used for the catalytic decomposition of the diazo compounds, the copper compounds have been deeply studied.[44−46]

The copper complexes examined in the present study are trinuclear, dinuclear, and mononuclear species, and the reaction studied has been the classical cyclopropanation of styrene by ethyl diazoacetate (EDA), which is reported in Scheme 4. In Table 4 we report the results of the reaction for the tested catalysts, comparing them with the results obtained for the reactions catalyzed by CuCl, one of the most studied catalysts.[44−46]

As far as the overall cyclopropanation yields are concerned, it is possible to see that only complex **2** gives a moderate result (51%) while the other complexes afford the cyclopropanated compounds with excellent yields, between 76% and 91%. Particularly interesting are the stereochemical

Table 4. *syn*:*anti* Molar Ratios and Yields (%, in Parentheses) for the Cyclopropanation Reaction of Styrene with EDA Catalyzed by Copper Catalysts

entry^a	catalyst	*syn*:*anti* molar ratios (overall yield)	entry^a	catalyst	*syn*:*anti* molar ratios (overall yield)
1	CuCl	0.6 (79.3)	5	**5**	0.41 (81.3)
2	**1**	1.64 (82.4)	6	**7**	0.66 (80.0)
3	**2**	1.24 (51.0)	7	**11**	0.51 (75.7)
4	**3**	1.28 (86.0)	8	**12**	0.57 (90.6)

^{a} Reactions were carried out at 60 °C in CHCl$_3$ with a molar ratio of substrate:EDA:catalyst = 2500:1000:1.

results, showing that the trinuclear complexes (**1**−**3**) afford better *syn*:*anti* ratios compared to the mononuclear and dinuclear derivatives. Moreover, among the trinuclear compounds, **1** gives an interesting *syn*:*anti* ratio of 1.64, which is not very easy to find in the literature[47−51] and represents a significant excess of the more hindered compounds, useful from the synthetic point of view. In our opinion such results are correlated to the fact that trinuclear derivatives present a more rigid structure which does not allow the substrates to approach the catalytic site in a random way, and this fact can be responsible for the stereochemical results. Further

(42) Dave, V.; Warnhoff, E. W. *Org. React.* **1970**, *118*, 217.
(43) Doyle, M. P. *Chem. Rev.* **1988**, *88*, 911.
(44) Evans, D. A.; Woerpel, K. A.; Hinman, M. M.; Faul, M. M. *J. Am. Chem. Soc.* **1991**, *113*, 726.
(45) Lowenthal, R. E.; Abiko, A.; Masamune, S. *Tetrahedron Lett.* **1990**, *31*, 6005.
(46) Pfaltz, A. *Acc. Chem. Res.* **1993**, *26*, 339.

(47) Callot, H. J.; Piechocki, C. *Tetrahedron Lett.* **1980**, *21*, 3489.
(48) Callot, H. J.; Metz, E.; Piechocki, C. *Tetrahedron* **1982**, *38*, 2365.
(49) O'Malley, S.; Kodadek, T. *Tetrahedron Lett* **1991**, *32*, 2445.
(50) Robbins Wolf, J.; Hamaker, C. G.; Djukic, J.-P.; Kodadek, T.; Woo, L. K. *J. Am. Chem. Soc.* **1995**, *117*, 9194.
(51) Maxwell, J.; Kodadek, T. *Organometallics* **1991**, *10*, 4.

studies on the reaction mechanism may elucidate this interesting point.

In conclusion, we have here shown that a new triangular trinuclear copper derivative, [$Cu_3(\mu_3$-OH)(μ-pz)$_3$(MeCOO)$_2$-(Hpz)] (**1**) has been obtained by reacting Hpz with Cu-(MeCOO)$_2 \cdot$H$_2$O. The spontaneous self-assembly seems to occur only when unsubstituted pyrazole is employed, as indicated by the fact that the reactions of copper(II) acetate with some substituted pyrazoles lead to the formation of mononuclear and dinuclear species. Also the presence of acetate ions seems to be determining for the formation of the trinuclear triangular arrangement, the formation of a mononuclear derivative being observed in the reaction of copper(II) trifluoroacetate with pyrazole.

Compound **1** has been fully characterized. It shows that the idealized 3-fold symmetry of the $Cu_3(\mu_3$-OH) core, roughly preserved by the μ_2-bridging pyrazolate units, is broken by the terminal ligands coordinated to the three Cu centers. In fact, while one Cu atom is coordinated by a terminal pyrazole, the other two Cu atoms bear acetate ligands but arranged in a different way around the metals. As a consequence, the three Cu atoms are nonequivalent and the molecule is asymmetric.

Trivial symmetry arguments allowed us to obtain useful information about the bonding scheme of the $Cu_3(\mu_3$-OH)

core of **1**, while a detailed assignment of the UV−vis absorption spectrum needed quantitative DFT calculations. The EPR spectrum of **1** indicates that its ground state corresponds, in agreeent with the μ_{eff} value of 2.156 μ_B, to a doublet state. Values of the g factor components computed for the state corresponding to $S = 1/2$ are in semiquantitative agreement with data obtained by the best fitting simulation of the EPR spectrum.

The triangular trinuclear compound **1** has been investigated as a catalyst precursor in the cyclopropanation reaction, showing an interesting selectivity toward the *syn* products, a feature opposite that normally reported.

Further investigations on the role of substituents on the azole and on the carboxylate chain effects are in progress.

Supporting Information Available: X-ray crystallographic files in CIF format for the structure determinations of **1** and **12**. This material is available free of charge via the Internet at http://pubs.acs.org.

IC049260Y